CO_2 hydrogenation to methanol with an innovative Cu/Zn/Al/Zr catalyst: experimental tests and process modeling

Giorgia Lombardelli[a,b], Mauro Mureddu[c†], Sarah Lai[c], Francesca Ferrara[c], Alberto Pettinau[c], Luciano Atzori[c,d], Antonio Conversano[a,b], Manuele Gatti[a*]

[a] *Politecnico di Milano, Dipartimento di Energia, Via Lambruschini 4, Milano 20156, Italy*

[b] *LEAP s.c. a r.l., Via Nino Bixio 27c, Piacenza 29121, Italy*

[c] *Sotacarbo S.p.A., Grande Miniera di Serbariu, Carbonia 09013, Italy*

[d] *Department of Chemical and Geological Sciences, University of Cagliari, 09042 Monserrato, Italy*

* *corresponding author. E-mail address: manuele.gatti@polimi.it*

† *corresponding author. E-mail address: mauro.mureddu@sotacarbo.it*

ABSTRACT

In this study, an innovative Cu/Zn/Al/Zr catalyst for the conversion of CO_2 and H_2 into methanol is tested at laboratory scale (0.5 g of catalyst into a cylindrical fixed bed reactor, with 9.1 mm internal diameter). Fourteen experimental tests are performed under isothermal conditions (T = 250 °C), covering a range of pressure (3.0-7.0 MPa), Gas Hourly Space Velocity (4,000-13,000 h^{-1}) and H_2/CO_2 molar ratio (between 3 and 6) relevant to industrial applications, with or without CO in the feed mixture, with flow-rates ranging between 200-650 NmL/min. Based on the established Graaf's kinetic model, new kinetic parameters are calibrated and a plug-flow model of the isothermal reactor is implemented and simulated in Aspen Plus. A reasonable agreement between experimental data and calibrated model is achieved, with deviations lower than 10% of the measured flow rates for each species in the product stream. CO_2 conversion up to 26% and methanol yields up to 13% are obtained during the test campaign (test run #12). The model represents a valid tool for future research or engineering studies targeting the design and performance assessment of demo/full-scale CO_2-to-methanol synthesis processes based on the Cu/Zn/Al/Zr catalyst introduced in this paper.

KEYWORDS:

CO_2 utilization; Methanol synthesis; Process Modeling; CO_2 hydrogenation; Cu/Zn/Al/Zr catalyst; Experimental test.

1. Introduction

Methanol (MeOH) is an important building block in chemical industry, since it is widely employed as an intermediate through which a lot of materials and everyday products are manufactured. It is mainly used for the production of olefins and as precursor in the synthesis of formaldehyde, that is at the base of the production process of some resins and various plastics [1]. Methanol also plays an important role in the transport fuels industries, not only for its use as gasoline blending, but also for its use in the production of biodiesel and in the synthesis of dimethylether (DME). Besides being a key and versatile molecule for the chemical industry, methanol takes advantage from its high energy density and liquid state at ambient conditions, which open the field to several new applications, such as directly as a fuel in heavy transport sectors (for example naval) or as an energy carrier [2]. In 2019 around 98 million tonnes (Mt) of methanol was produced with a worldwide annual demand nearly doubling over the past decade [3]. The future outlook points towards a further growth in methanol global demand: it is estimated that methanol production will reach more than 120 Mt by 2025 and 500 Mt in 2050 [3]. Nowadays, about 65% of methanol is industrially produced from natural gas reforming and subsequent catalytic conversion of syngas, while the remaining 35% is mainly based on coal gasification [3]. In industrial applications, the conversion of syngas into methanol is supported by commercial catalysts based on copper (Cu), zinc oxide (ZnO) and alumina (Al_2O_3) and occurs according to three simultaneous reactions: the carbon monoxide hydrogenation (Eq. (1)), the Reverse Water-Gas Shift (RWGS) reaction (Eq. (2)) and the carbon dioxide hydrogenation (Eq. (3)).

$$CO + 2H_2 \rightleftharpoons CH_3OH \qquad \Delta H^0_{R(298K)} = -90.7\ kJ\ mol^{-1} \qquad (1)$$

$$CO_2 + H_2 \rightleftharpoons CO + H_2O \qquad \Delta H^0_{R(298K)} = +41.2\ kJ\ mol^{-1} \qquad (2)$$

$$CO_2 + 3H_2 \rightleftharpoons CH_3OH + H_2O \qquad \Delta H^0_{R(298K)} = -49.4\ kJ\ mol^{-1} \qquad (3)$$

Some side reactions can occur and lead to the formation of several byproducts, as for example light hydrocarbons [4], however the formation of by-products is usually limited thanks to the high selectivity of the catalyst and the choice of suitable operating conditions. The operating conditions of the industrial scale catalytic reactors for the methanol synthesis are typically around 220–270 °C and 5.0–10.0 MPa [4].

The increasing demand of renewable fuels and the need to substitute the fossil sources with raw materials featuring a low or zero-carbon footprint, encourages the research of alternative non-fossil pathways for the production of methanol. For this reason, there is a growing interest around the direct CO_2 hydrogenation to methanol process [5,6], where the feedstocks are either captured or biogenic CO_2, which supplies the carbon content, and “green” H_2 (for example produced from decarbonized pathways such as electrolysis fed by renewable sources) which provides not only the hydrogen atoms specified by the reaction stoichiometry, but

also the significant chemical energy input required to convert the highly stable carbon dioxide molecule [7]. Although CO_2 is a stable and inert molecule, which makes it very challenging and energy-intensive to be converted into more useful reduced forms, CO_2 hydrogenation is a particularly attractive process when CO_2 is not generated on purpose but captured from industrial [8–10] or biogenic [11–13] flue gases. Methanol production from CO_2, made available by capture technologies, and renewable-derived hydrogen is one of the most interesting CO_2 utilization applications, with a non-negligible potential in terms of greenhouse gas mitigation contribution [14], since the estimated CO_2-to-methanol potential market is of the order of 5-50 Mt_{CO2}/y in 2030 [15]. Currently, there is only one commercial CO_2-to-methanol plant in operation, the George Olah plant [16]. It operates in Iceland since 2012, managed by Carbon Recycling International (CRI), and it produces approximately 4000 t/y of methanol by combining CO_2 captured from the exhaust of a geothermal power plant and H_2 generated from water electrolysis using geothermal electricity [17]. Moreover, as reported by IRENA study about Renewable Methanol [3], CRI is designing for the near future new CO_2-to-methanol production plants in China and Norway and many facilities are planned around the world from other technology providers. In addition, several R&D (Research and Development) projects, recently reviewed by Dieterich et al. [18], are ongoing, in order to demonstrate and optimize the production of methanol via direct CO_2 hydrogenation, aiming at increasing catalyst productivity while also reducing methanol production costs, which are still the main barrier to the commercial development of this technology compared to the fossil fuel reforming or gasification-based route.

In the methanol synthesis through CO_2 hydrogenation the H_2/CO_2 stoichiometric ratio is equal to 3; a ratio higher than 3 indicates that there is an excess of H_2 in the feed gas, while a lower value means that there is an excess of carbon. Otherwise, the methanol synthesis starting from CO-based-syngas requires a CO/H_2 ratio equal to 2 for stoichiometric conditions. Compared to the conventional syngas-to-methanol process, the CO_2 hydrogenation requires more hydrogen for unit of carbon, resulting in a larger amount of water formed as by-product of the methanol synthesis reaction. Moreover, the direct CO_2 hydrogenation route results in lower methanol yield; in presence of higher amount of CO_2, the RWGS reaction produces larger amounts of water (see Eq. (2)), thereby forcing the equilibrium of the hydrogenation reaction towards lower amounts of methanol (see Eq. (3)), which is more shifted towards the reactants side. A consequence of the greater water production during the CO_2 hydrogenation compared to the syngas-to-MeOH process is the possible deactivation of the traditional Cu/ZnO-based catalysts [19], mainly due to the agglomeration of ZnO species and the oxidation of metallic Cu [20]. To the deactivation obstacle it is also added the low activity and methanol selectivity (due to

the RWGS reaction) [21] of the commercial catalyst of methanol synthesis in presence of direct CO_2 hydrogenation.

In order to increase the stability of the catalyst for methanol synthesis, scientific research focuses on replacing traditional $Cu/ZnO/Al_2O_3$ catalysts with new catalysts presenting at the same time good activity towards CO_2 and high selectivity to methanol [22,23]. The Cu/ZnO-based catalysts remain the most studied materials [22], [24,25], with the addition of different selected oxides, such as ZrO_2, Ga_2O_3, In_2O_3, PdO, or a combination of more than one oxides [21,26,35,36,27–34]. Particularly, copper-based zirconia-containing catalysts exhibit promising results [22], [32], also thanks to its high stability [37]. The catalyst stability during CO_2 hydrogenation was investigated by Li et al. [30], that compared the performances of a traditional $Cu/ZnO/Al_2O_3$ catalyst and two Zr-doped catalysts; over almost 100 h of operation the $Cu/ZnO/ZrO_2/Al_2O_3$ catalyst maintained a constant activity, by contrast, conventional $Cu/ZnO/Al_2O_3$ showed gradual decrease in methanol yield. Finally, the three catalysts performances were studied via experimental tests in a tubular fixed bed reactor (inner diameter of 8 mm) for the methanol synthesis at 230 °C and 3.0 MPa, in once-through configuration. The $Cu/ZnO/ZrO_2/Al_2O_3$ catalyst, with a CO_2 conversion of 23.2% and a selectivity of 60.3, showed a better catalytic activity than the $Cu/ZnO/ZrO_2$ (CO_2 conversion=19.3% and CH_3OH selectivity=49.6%) and $Cu/ZnO/Al_2O_3$ (CO_2 conversion=18.7% and CH_3OH selectivity=43%) catalysts. Also Lim et al. [38] studied the performance of a $Cu/ZnO/Al_2O_3/ZrO_2$ catalyst, in an isothermal tubular fixed bed reactor (with a diameter of 10.2 mm and a catalyst loading of 1 g), at 5.0 MPa and temperatures ranging between 230 and 280 °C, with space velocity (SV) equal to 2,000−6,000 mL g_{cat}^{-1} h^{-1}; during experimental tests, a maximum CO_2 conversion of around 30% was achieved. Mureddu et al. [39]investigated the effect of zirconium and/or ceria in Cu/Zn/Al based catalytic performance. Tests were carried out at 250 °C, 3.0 MPa and with a Gas Hourly Space Velocity (GHSV) of 12,000 NmL g_{cat}^{-1} h^{-1};results showed that Cu/Zn/Al/Zr material had the best performance in terms of CO_2 conversion (18.7 %), and methanol space time yield (250 $mg_{CH3OH}g_{cat}^{-1}h^{-1}$).

On the basis of the above-mentioned experimental outcomes, the Cu/Zn/Al/Zr catalyst prepared by Mureddu et al. [39] has been chosen for a more detailed study, focusing on the analysis of the catalytic activity for a wide range of operating conditions, including also tests with CO as input, and aiming at calibrating the kinetic model parameters to support future process simulation studies. The experimental and modeling activities reported in this paper represents an original contribution to this area and could be useful to enable the selection of optimized reactors and process conditions for CO_2 hydrogenation to MeOH based on the Cu/Zn/Al/Zr catalyst from this study. Most of the literature studies about new catalysts for CO_2 hydrogenation

are of experimental nature, however for few catalysts only modeling activities and kinetic parameters calibration are carried out [35,40]. Moreover, several experimental studies are limited to the catalyst performance analysis under fixed operating conditions or by investigating the impact of only temperature or pressure [21,27,30,41]. Only a very limited number of cases evaluate the behavior of the catalyst both with $CO_2 + H_2$ or with a mixture of $CO + CO_2 + H_2$ in the reactants [35,38]. Tests with CO in input are significant as CO is produced in the methanol synthesis reactor from CO_2 reduction and in a full-scale design a significant fraction of the effluent gases is recirculated at the reactor inlet in order to increase the yield of the process. Experimental data covering a wide range of operating conditions with both CO_2 and CO in input are required to characterize the activity of the catalyst and develop a calibrated model able to describe methanol reactor performance. The definition of a calibrated kinetics model describing the catalytic activity in the expected range of operation is crucial to support process designs, simulations and Techno-Economic Assessments (TEA) of methanol synthesis technologies for up-scaling of large-scale technology development [19].

In the present study the innovative Cu/Zn/Al/Zr catalyst for methanol synthesis via CO_2 hydrogenation is tested at laboratory scale and its kinetic behavior is modeled. The catalyst performances are investigated through fourteen experimental tests at different conditions: pressure, composition of the inlet reactants and Gas Hourly Space Velocity. The tests results are used for the calibration of a plug-flow reactor model, suitable to carry out future process studies for up-scaling and technology benchmarking purposes with commercial simulation software such as Aspen Plus.

2. Experimental methods

2.1. Catalyst formulation and characterization

The catalyst preparation method and physicochemical characterization in terms of composition, texture, structure, surface acidity and basicity, and reducibility is reported in detail in a previous paper by Mureddu et al. [39] and it is briefly summarized in the following. For the Cu/Zn/Al/Zr catalyst an aqueous solution (100 cm^3) with a total concentration equal to 1.5 M (molar) containing appropriate amounts of $Cu(NO_3)_2$, $Al(NO_3)_3$, $Zn(NO_3)_2$ and $ZrO(NO_3)_2$ was first prepared. A second solution containing 7.15 g of Na_2CO_3 and 13.95 g of NaOH in 100 cm^3 of distilled water, was then slowly added to the former one, at room temperature and under stirring, by using a peristaltic pump, which allowed the flow rate to be adjusted in order to maintain the pH constant and equal to 11. The solution was kept at 60 °C for 20 h, the resulting hydrotalcite was dried at 80 °C

overnight and finally calcined at 500 °C for 4 h in order to obtain the corresponding mixed oxide composition: 2Cu_1Zn_0.7Al_0.3Zr.

2.2. Experimental setup and tests

Catalytic tests were carried out in a customized Microactivity Effy (PID Eng&Tech) bench-scale plant reported in *Figure 1*, where the schematic diagram of the lab-scale facility and a photo of the reactor box are depicted. The facility (*Figure 1* a) includes gaseous reactants feeding and mixing area, a thermostated reactor, collection area and separation between condensable and non-condensable products and the zone of depressurization and measure of the outgoing gaseous flow subsequently sent to the to the analyzer. Feed mixture preparation (including both pure gases and mixtures) is carried out with six independent gas lines with dedicated mass flow controllers: Bronkhorst "Mini Cori Flow" for CO_2 and mixture stream with an accuracy of ± 0.2% of reading and Bronkhorst "El-Flow" for CO, H_2 and N_2 with an accuracy of ± 0.5% of reading. The reaction zone, located inside a hot-box (*Figure 1* b), comprises the reactor, the gas supply lines and the discharge line of the products stream. The oven is heated and thermostated for temperature control purposes.

Pressure control is based on a high-speed precision servo-controlled valve with an accuracy of ± 0.1 bar. Downstream the hot-box there is the collection and separation area where the unreacted gaseous products are separated from hydrophilic and hydrophobic liquid products. The unreacted gaseous products and inert gases that may be present are depressurized and their flow rate is measured. Between the pressure controller and regulator and the volumetric flow meter, a coalescing filter is located to protect the outgoing flow meter and the gas chromatograph.

The high-pressure fixed bed stainless steel reactor (9.1 mm internal diameter, an external diameter of 14.3 mm and a total external length of 304.8 mm) already described by Mureddu et al. [42] is used. A porous plate (made of Hastelloy C, 20 μm) and quartz wool were used to support the catalytic bed inside the isothermal temperature zone of the reactor (catalyst bed of 50 mm in length and 3.1 cm^3 in volume). The reactor, inserted in a vertical electric oven that allows it to operate in quasi-isothermal conditions, was loaded with 0.5 g of Cu/Zn/Al/Zr catalyst diluted with 2.5 g of α-Al_2O_3. Before the tests, the catalyst is reduced *in-situ* by flowing a H_2/N_2 mixture (H_2, 15%vol) at 250 °C for 2 h under atmospheric pressure. Then, the reactants mixture (with composition, defined according to Table 1) is sent to the reactor and the temperature is kept constant at 250 °C for all the experiments. Catalyst activity was measured at pressures ranging from 3.0 to 7.0 MPa. Each run was held for 6 h in the same operating condition in order to reach a stationary catalytic behavior.

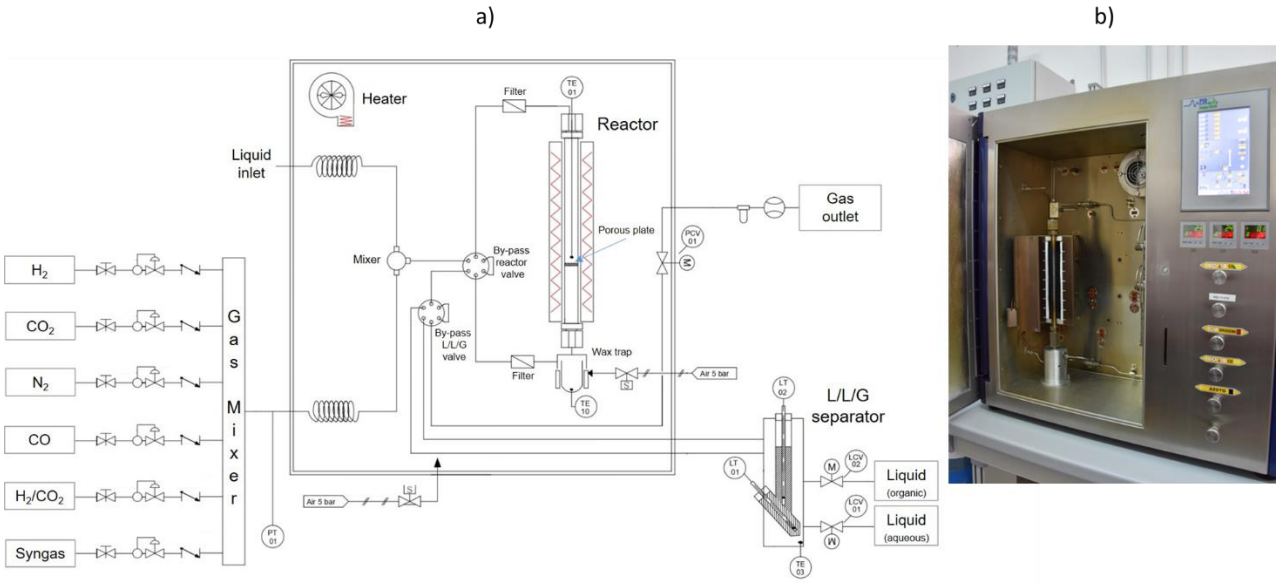

Figure 1: Scheme of the experimental facility (a) and photo of the reactor hot-box (b).

The products stream leaving the reactor box is analyzed by means of a gas chromatograph (Agilent 7890B, Santa Clara, California, CA, USA) equipped with a flame ionized detector (FID) for carbon-containing compounds and with a thermal conductivity detector (TCD) for permanent gases. Two columns connected in series are used to identify the components of the outlet gas mixture. In particular, CO_2, methanol, dimethyl ether, ethane, and propane are separated by a HP-Plot Q (Agilent) column (length 30 m, inner diameter 0.53 mm, film thickness 40 μm), while a HP-PLOT Molesieve (Agilent) column (length 30 m, inner diameter 0.53 mm, film thickness 50 μm) is used for H_2, N_2, CH_4, and CO. To avoid condensation of condensable products, the connection lines between the plant gas outlet and gas chromatograph inlet are heated at 180 °C.

A wide range of operating conditions are covered in order to investigate the effect of different gas mixtures on the catalytic performance and to calibrate the kinetic model. As shown in Table 1, the H_2/CO_2 molar ratio was fixed to stoichiometry value of 3 mol mol^{-1}, except for tests #6 and #12 where a ratio of 3.9 and 6.0 mol mol^{-1} was used, respectively. Another exception are tests #13 and #14 also including CO in input and for which a $H_2/(CO_2+CO)$ molar ratio equal to 2.2 and 3.1 mol mol^{-1} is chosen. Pressures between 3.0 and 5.5 MPa are tested and Gas Hourly Space Velocity ranges between 4,000 and 13,000 h^{-1} (with fixed catalyst loading and by varying the inlet flowrate). In order to ensure the repeatability of the analysis, all the catalytic tests are repeated three times under the same conditions and the estimated relative standard deviations for the conversion of CO_2 is in the range of 2-5%.

Table 1: Operating conditions of the experimental tests performed at 250 °C.

				Reactants composition				
Test ID #	Pressure (MPa)	GHSV (h^{-1})	Flow rate of reactants (NmL min^{-1})	H_2 ($\%_{vol}$)	CO_2 ($\%_{vol}$)	CO ($\%_{vol}$)	N_2 ($\%_{vol}$)	Stoichiometric ratio at reactor inlet: $H_2/(CO+CO_2)$
1	3.0	4,000	200	50.1	16.8	0	33.1	3.0
2	3.0	7,008	350	67.4	22.6	0	10.0	3.0
3	3.0	7,020	351	50.0	16.7	0	33.3	3.0
4	3.0	6,960	348	33.1	11.0	0	55.9	3.0
5	3.0	7,000	350	50.0	16.7	0	33.3	3.0
6	3.0	7,000	350	49.9	12.9	0	37.2	3.9
7	3.0	10,000	500	49.9	16.7	0	33.5	3.0
8	3.0	12,980	649	50.2	16.9	0	32.9	3.0
9	5.0	7,004	350	39.3	13.2	0	47.5	3.0
10	5.0	6,544	327	60.2	20.3	0	19.5	3.0
11	5.4	6,544	327	60.2	20.3	0	19.5	3.0
12	6.8	6,990	350	50.4	8.4	0	41.2	6.0
13	6.5	7,000	350	61.1	11.8	15.4	11.7	2.2
14	6.5	10,000	500	66.6	8.7	12.9	11.8	3.1

3. Modeling

The laboratory reactor presented in section 2.2 is modeled as an isothermal pseudo-homogeneous one-dimensional Plug Flow Reactor (PFR), according to the same methodology proposed by Lim et al. [28], Portha et al. [30] , Atsonios et al. [34] and Battaglia et al. [35]. The following assumptions are considered along the reactor: isothermal conditions, no pressure drop, stationary conditions, uniform conditions on each cross section (no radial gradients) and negligible mass-transfer limitations.

The reactor is modeled with the process simulation software Aspen Plus v10.0, using the RPlug unit operation block, and adopting the Peng-Robinson Equation of State to calculate the fugacities of the chemical species involved. A single tube reactor with the same geometry and catalyst loading as from the experimental apparatus is simulated. The key chemical reactions involved in methanol synthesis, reported in Eqs. (1), (2) and (3), are computed according to the kinetic model proposed by Graaf [45] and recently applied by Portha et al. [40] and Nestler et al [19]. This approach is consistent with other recent works focused on the kinetic modeling of other innovative catalysts for CO_2 hydrogenation in fixed-bed reactors [35,40,46], which confirmed the applicability of Graaf's kinetic model [45], provided that its kinetic parameters, such as the pre-exponential factors and the activation energies, are tuned according to the experimental data of the catalyst under

investigation. The Graaf's kinetic model was originally developed to describe the methanol synthesis over a commercial $Cu/ZnO/Al_2O_3$ catalyst from synthesis gas and it is based on a dual-site Langmuir-Hinshelwood-Hougen-Watson mechanism (LHHW), simultaneously considering CO and CO_2 hydrogenation and the water-gas shift reactions [47]. The mathematical formulation for the computation of the rate of reactions for CO hydrogenation ($r_{CH_3OH,CO}$), reverse water-gas shift (r_{H2O}), and CO_2 hydrogenation ($r_{CH_3OH,CO2}$) are reported in Eq. (4), Eq.(5) and Eq.(6), where k_{ps1}, k_{ps2}, k_{ps3} are the kinetic constants of the reactions, K_{CO}, K_{CO2}, $K_{H2O}/K_{H2}^{1/2}$ the adsorption equilibrium constants of CO, CO_2, H_2O and H_2, K_{p1}, K_{p2}, K_{p3} the equilibrium constants and f the fugacity (linked to the partial pressure through the fugacity coefficient) of the components involved in the reactions [45].

$$r_{CH_3OH,CO} = \frac{k_{ps1}K_{CO}[\, f_{co}f_{H2}^{3/2} - f_{CH3OH}/(f_{H2}^{1/2}K_{p1})]}{(1 + K_{CO}f_{CO} + K_{CO2}f_{CO2})[f_{H2}^{1/2} + \left(K_{H2O}/K_{H2}^{1/2}\right)f_{H2O}]} \quad (4)$$

$$r_{H2O} = \frac{k_{ps2}K_{CO2}[\, f_{co2}f_{H2} - f_{H2O}f_{CO}/K_{p2}]}{(1 + K_{CO}f_{CO} + K_{CO2}f_{CO2})[f_{H2}^{1/2} + \left(K_{H2O}/K_{H2}^{1/2}\right)f_{H2O}]} \quad (5)$$

$$r_{CH_3OH,CO2} = \frac{k_{ps3}K_{CO2}[\, f_{co2}f_{H2}^{3/2} - f_{CH3OH}/(f_{H2}^{3/2}K_{p3})]}{(1 + K_{CO}f_{CO} + K_{CO2}f_{CO2})[f_{H2}^{1/2} + \left(K_{H2O}/K_{H2}^{1/2}\right)f_{H2O}]} \quad (6)$$

This kinetic model is implemented in Aspen Plus v10.0 where the mass and energy balances are calculated at steady-state for the isothermal isobaric reactor. The kinetic constants are formulated according to the classical Arrhenius type eq. (7), where A_{ps} is the pre-exponential term, E_a in the activation energy, T the absolute temperature and R is the ideal gas constant.

$$k_{ps} = A_{ps}\exp\left(-\frac{E_a}{RT}\right) \quad (7)$$

The values of these constants are strictly related to the catalytic activity as well as to the specific operating conditions of the catalytic reactor, therefore they must be determined from experimental tests, in order to properly model the kinetic behaviour of the innovative catalyst proposed in this work [19,40]. For this reason, the pre-exponential term and the activation energies for the three reactions are calibrated and tuned to the specific catalyst studied in this work by minimizing the differences between experimental and modeling results according to the numerical methodology described in section 3.1. The equilibrium constants and the adsorption equilibrium constants are kept unchanged compared to those fitted by Graaf [8,48] and are expressed as a function of temperature according to the form $lnK = A + \frac{B}{T}$. This is in line with the approach

followed by other studies [38,40,47,49], since they depend on temperature only but not on the catalytic activity. The assumed values are reported in Table 2.

Table 2: Values of the constant A and B in the equilibrium constants and adsorption equilibrium constants for the reaction of CO_2 hydrogenation, RWGS and CO hydrogenation.

Constants	*A*	*B*	Ref.
K_{p1} [Pa^{-2}]	- 52.087 [Pa^{-2}]	11833 [K]	[48]
K_{p2} [-]	4.672 [-]	- 4773 [K]	
K_{p3} [Pa^{-2}]	- 47.415 [Pa^{-2}]	7060 [K]	
K_{CO}[Pa^{-1}]	- 22.256 [Pa^{-1}]	5629 [K]	[8]
K_{CO2} [Pa^{-1}]	- 25.678 [Pa^{-1}]	7421 [K]	
$K_{H2O}/K_{H2}^{1/2}$ [$Pa^{-0.5}$]	- 24.628 [$Pa^{-0.5}$]	10103 [K]	

3.1. Model calibration procedure

The numerical model developed in Aspen Plus was calibrated in order to fit the simulation results to the experimental data. Based on the kinetic expressions described in section 3, six parameters of the model were calibrated: the pre-exponential factor A_{ps} and activation energy E_a in the kinetic rate constants (eq. (7)) for the three reactions involved in methanol synthesis. The calibration was achieved by minimizing the discrepancy between the results of the fourteen experimental tests and the numerical simulation [47]. The Error Function (EF) that is minimized during calibration is a total sum of square as defined in Eq. (8), where *m* is the number of tests, $n_{i,exp}$ are the molar flow rates of CO_2, CO and CH_3OH at the outlet of the lab-scale reactor during the experimental tests and n_{sim} are the corresponding flow rates calculated from the simulation. The flow rates of each species (i) at the outlet of the reactor, $n_{i,exp}$, is calculated from experimental data according to Eq. (10) where n_{in} is the total molar flow rate entering the reactor, $x_{i,out}$ is the molar concentration of components (i) measured in the outlet flow (*Table 3*), $x_{N2,in}$ is the concentration of N_2 at reactor inlet (*Table 1*). Nitrogen is present in all cases and, although acting as an inert, is used for accurate flow-rates reconciliation purposes (as from Eq. (10) the flow rate of each species is normalized to the flow-rate of N_2 which is constant across the reactor), according to the internal standard method [50].

$$EF = \sum_{i=1}^{m} (n_{CO2,sim} - n_{CO2,exp})^2 + (n_{CO,sim} - n_{CO,exp})^2 + (n_{CH3OH,sim} - n_{CH3OH,exp})^2 \quad (8)$$

$$n_{i,exp} = n_{in} \cdot {}^{x_{N2,in}}/_{x_{N2,out}} \cdot x_{i,out} \quad (9)$$

Model calibration is performed by coupling an *ad hoc* Matlab R.2020b error minimization routine with Aspen Plus simulations. The minimization algorithm, schematized in *Figure 2*, works as follows: for a given set of model parameters, Matlab calls Aspen Plus to simulate the mass and energy balances for each test conditions, then the Aspen Plus simulation results (n_{sim}) are processed and compared by Matlab against the experimental data (n_{exp}), and the error function (*EF*) is computed. The model parameters were iteratively changed by the Matlab routine until the minimum error was obtained. For the EF minimization procedure in Matlab, the *fmincon* function based on the numerical algorithm 'interior-point' was used.

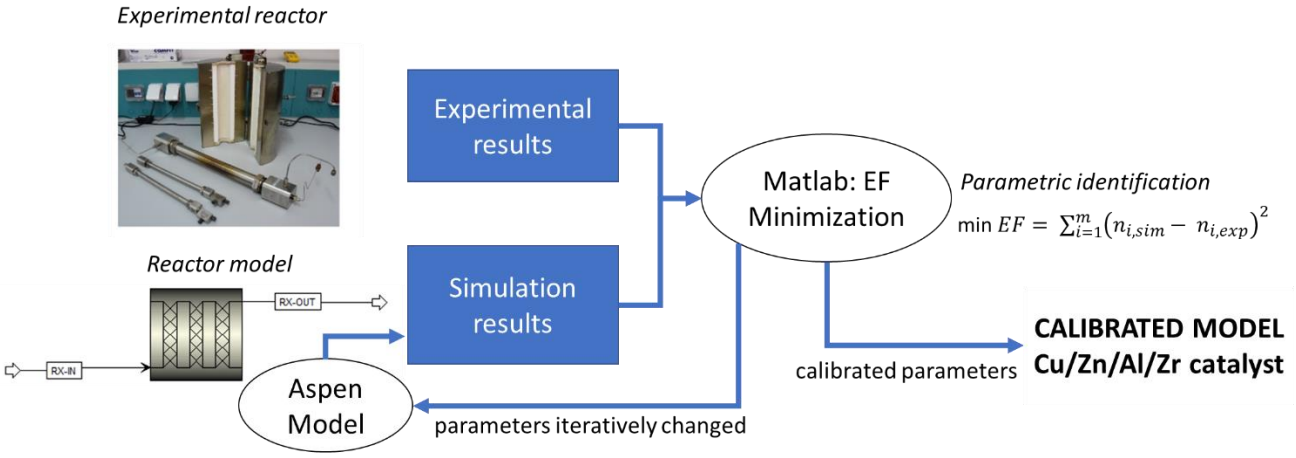

Figure 2: Numerical model calibration procedure.

4. Results and discussion

4.1. Experimental Results

During each test run, the composition of the outlet flow is measured by gas chromatographs as described in section 2.2. The molar compositions of CO_2, CO, CH_3OH, H_2 and N_2 from fourteen experimental tests are reported in Table 3. The presence of other hydrocarbons (methane, propane, ethane, dimethyl-ether) detected via GC is negligible (of the order of magnitude of 10 ppmv). Tests #1 to #12 are focused on CO_2 hydrogenation at different values of pressure, GHSV and H_2/CO_2 ratio. Tests #13 and #14 concern methanol synthesis with recycle or from a syngas stream including $CO/CO_2/H_2$. The overall tests duration varies in the range 5 - 22 hours.

Table 3: Experimental results from methanol synthesis tests at lab scale (input conditions reported in Table 1, T=250 °C; P=3.0 - 7.0 MPa; GHSV=7,000-13,000 h^{-1}): composition measured by gas chromatograph (average on the whole time on stream) at reactor outlet.

Test ID#	CO_2 (%mol)	CO (%mol)	CH_3OH (%mol)	H_2 (%mol)	N_2 (%mol)	H_2O (%mol)
1	14.5	1.8	0.77	46.7	33.6	2.63
2	20.6	1.4	1.04	64.2	10.2	2.56
3	15.1	1.2	0.67	47.5	33.7	1.83
4	9.7	1.0	0.32	31.4	56.3	1.28
5	15.0	1.3	0.65	47.4	33.7	1.95
6	11.3	1.1	0.61	47.5	37.7	1.79
7	15.4	0.9	0.55	47.9	33.8	1.45
8	15.9	0.7	0.48	48.6	33.2	1.12
9	11.4	1.2	0.73	36.5	48.2	1.97
10	17.9	1.5	1.36	56.3	20.0	2.94
11	17.9	1.5	1.44	56.1	20.0	3.06
12	6.3	1.1	1.16	47.0	42.1	2.34
13	11.4	14.6	1.47	59.5	12.0	1.03
14	8.0	12.3	1.11	65.5	11.9	1.19

Starting from the experimental results and test conditions summarized in *Table 1* and Table 3, the conversion of CO_2 and methanol yield are computed. Carbon dioxide conversion (X_{CO2}) and methanol yield (Y_{CH3OH}) are calculated according to equation (10) and (11), where $x_{CH3OH,out}$, $x_{CO2,out}$ and $x_{N2,out}$ are the concentration of methanol, CO_2 and N_2 measured in the outlet flow (*Table 3*) and $x_{CO2,in}$, $x_{CO,in}$ and $x_{N2,in}$ are the concentration of CO_2, CO and N_2 at the reactor inlet (*Table 1*). This approach, called internal standard method [50,51], takes advantage of the fact that the molar flow of nitrogen does not change between reactor inlet and outlet and that molar concentrations are measured with a greater accuracy (by the GC) than molar flow rates.

$$X_{CO2} = \frac{{}^{x_{CO2,in}}/_{x_{N2,in}} - {}^{x_{CO2,out}}/_{x_{N2,out}}}{{}^{x_{CO2,in}}/_{x_{N2,in}}} * 100 \qquad (10)$$

$$Y_{CH3OH} = \frac{{}^{x_{CH3OH,out}}/_{x_{N2,out}}}{{}^{x_{CO2,in}}/_{x_{N2,in}} + {}^{x_{CO,in}}/_{x_{N2,in}}} * 100 \qquad (11)$$

The experimentally derived values of carbon dioxide conversion and methanol yield are reported in *Table 4* and Figure 3. Test #12, carried out at the highest pressure (7.0 MPa) and with a H_2/CO_2 ratio equal to 6, hence with large hydrogen excess, reports the greatest CO_2 conversion (26%) and CH_3OH yield (13.5%). For all the remaining test conditions, CO_2 conversion ranges between 6 and 15%, while the methanol yield is

comprised between 2.8 and 6.9%. These are all results in line with typical literature ranges for similar catalysts for methanol synthesis from pure CO_2, with once-through conversion values reported by the modeling work of Nestler et al. [19] (at 250 °C, P = 5 MPa, GHSV= 20000 h^{-1}, stoichiometric number = 2) close to 15% at the equilibrium and ranging between 7 and 13% for commercial catalysts. Test results can be interpreted by highlighting the following impact of parametric variations:(i) the GHSV increase from test #1 to #2 and from #6 to #7 and #8 causing a decrease in methanol yield; (ii) the CO_2 partial pressure increases from test #2 (p_{CO2}= 0.7 MPa) and to #3 and #4 (p_{CO2}= 0.5 and 0.3 MPa) and from test #10 to #11 (with a total pressure increase of 5 bar) which enhances methanol yield; (iii) the H_2/CO_2 ratio increases from test #3 to #6 causing an increase in methanol yield.

Tests #3 and #5 were conducted under the same operating conditions, in order to prove the replicability and reliability of tests. Test runs #13 and #14 are carried out at higher pressures (65 bar) and by adding CO to the inlet stream, which is never present in the reactant streams of trials #1 to #12.

Table 4: Key performance indicators calculated from test results: Carbon dioxide conversion (X_{CO2}) and methanol yield (Y_{CH3OH}).

Test ID #	X_{CO2} (%)	Y_{CH3OH} (%)
1	15.2	4.5
2	10.8	4.5
3	11.1	3.9
4	11.8	2.9
5	11.3	3.8
6	13.3	4.6
7	8.6	3.3
8	6.8	2.8
9	14.4	5.5
10	13.8	6.5
11	14.3	6.9
12	26.2	13.5
13	5.8	5.3
14	8.4	5.1

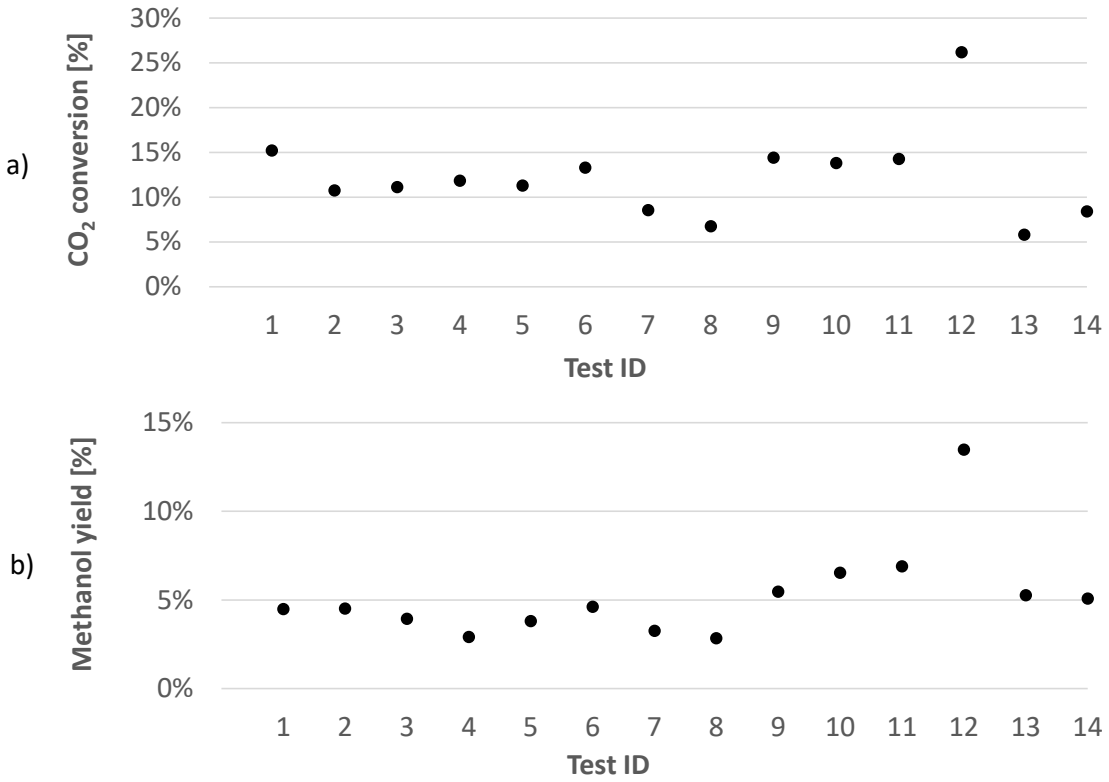

Figure 3: The conversion of carbon dioxide (a) and the methanol yield (b) resulting from experimental tests.

Figure 4, *Figure 5* and *Figure 6* highlight of the behavior of methanol yield as a function of key test conditions and comparison against the maximum theoretical conversion value predicted by the equilibrium for each case is reported. As expected, high total pressures, high H_2 to CO_2 ratios and low GHSV lead to increased methanol yields. To gain insight into the relationship between the performance of the catalyst and the operating conditions, the effects of the following process variables are highlighted: (i) pressure, (ii) the H_2/CO_2 ratio and (iii) GHSV. *Figure 4* shows the pressure influence from tests #2, #3 and #4, since the partial pressure of H_2 and CO_2 is decreased by increasing the amount of N_2 in the input flow at given total pressure (3 MPa). When CO_2 partial pressure is reduced from 0.7 to 0.3 MPa under the same H_2/CO_2 ratio equal to 3, the methanol yield decreases by 30% as shown in *Figure 4*.

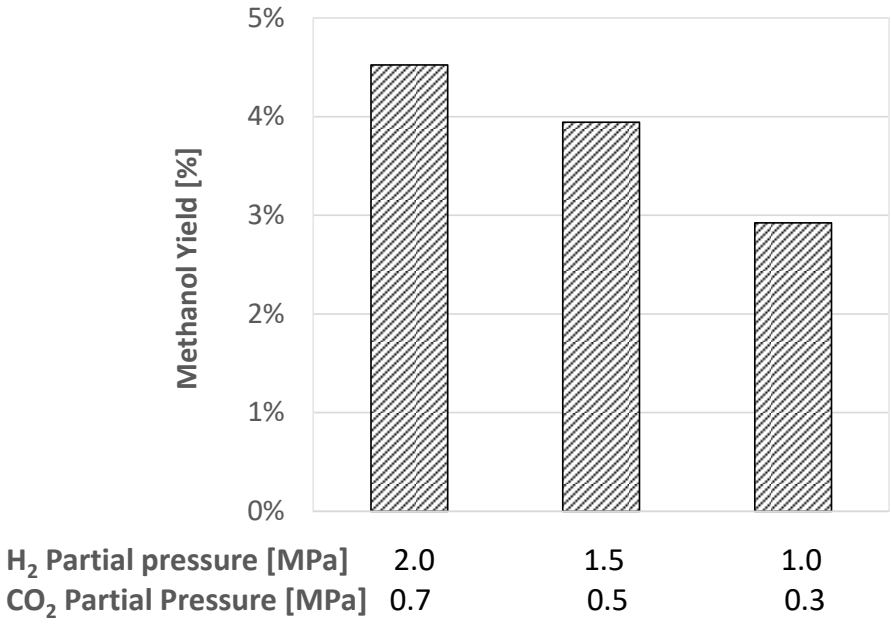

Figure 4: Methanol yield resulting from experimental tests #2, #3 and #4 for different values of H_2 and CO_2 partial pressure (T=250 °C; GHSV=7,000 h^{-1}; H_2/CO_2=3).

Figure 5 shows the positive effect on the catalytic performance following an increase in the H_2 excess, since if the H_2/CO_2 ratio grows from 3 to 3.9 under the same operating conditions the yield increases by 15% (from 4% to 4.6%) thanks to the shift of the equilibrium towards the formation of the products, as foreseen by Le Chatelier's principle.

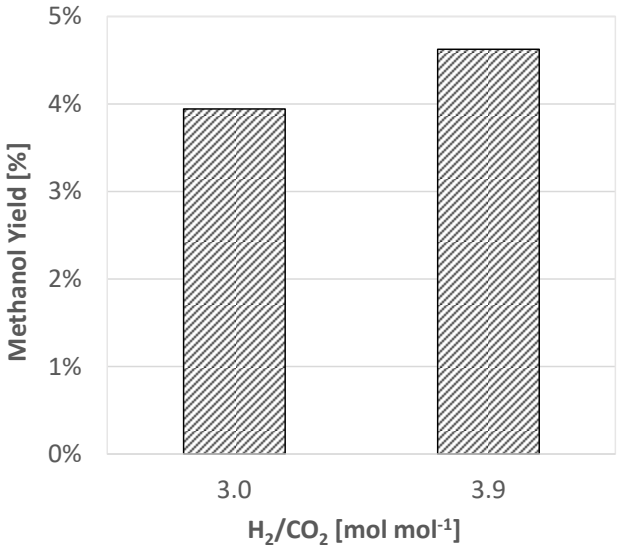

Figure 5: Methanol yield carried out from experimental tests 3 and 6 for different values of H_2/CO_2 ratio (T=250 °C; P=3.0 MPa; GHSV=7,000 h^{-1}).

Figure 6 reports the effect of a GHSV change as investigated in tests #1, #5, #7 and #8. while also highlighting the expected theoretical yield under equilibrium condition. The value of the methanol yield at equilibrium is obtained via chemical equilibria simulation with the "RGibbs" Aspen Plus model based on Gibbs free energy minimization at the same inlet conditions from the analyzed test runs. It is worth noting that GHSV does not affect the equilibrium conditions and for this reason a horizontal equilibrium profile is reported in *Figure 6*. A variation of the GHSV from 4,000 to 13,000 h^{-1} leads to a decrease of the residence time in the experimental reactor and therefore a decrease of the methanol yield, varying in the range 4.5% - 2.8%, with respect to the equilibrium value equal to 5.6%.

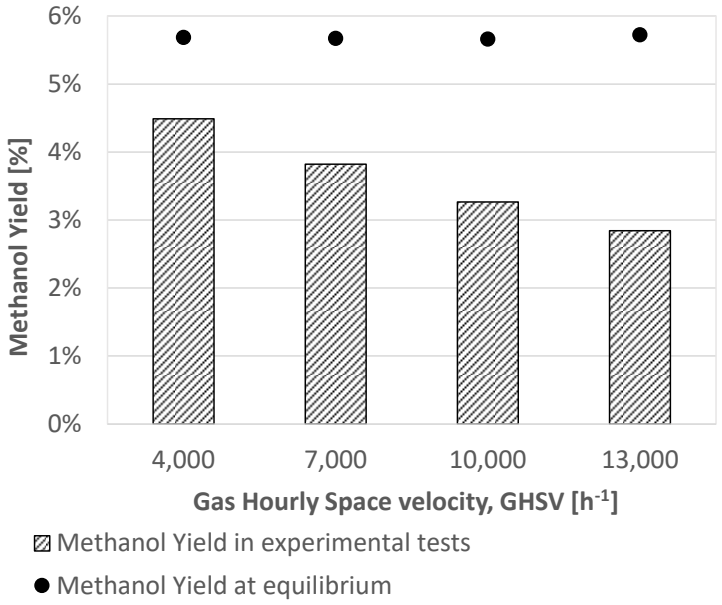

Figure 6: Methanol yield Y at equilibrium and resulting from experimental tests #1, 5, 7 and 8 as function of the Gas Hourly Space Velocity (T=250 °C; P=3.0 MPa; H_2/CO_2=3).

4.2. Model Calibration Results

The proposed numerical plug-flow model of the reactor, under steady-state conditions, isothermal/isobaric conditions, no axial dispersion, is calibrated on the basis of the results of fourteen experimental tests. The kinetic model parameters are determined by minimizing the sum of square Error Function, in Matlab, between experimental and simulations flow rates for the following species: CO_2, CO and CH_3OH. *Table 5* summarizes the calibrated values of the pre-exponential factor (A_{ps}) and the activation energy (E_a) for the synthesis reactions (1), (2) and (3). Numerical values of both parameters are of the same order of magnitude of the ones reported by Graaf for a commercial catalyst and similar results are found in the literature with other innovative catalysts for CO_2 hydrogenation (as for example in Portha et al. [40]). Concerning the

CO_2 hydrogenation reaction, a slight increase of the kinetic parameter was observed between this new catalyst and Graaf's one: as shown in *Figure 7* the increase of the pre-exponential term and a marginal reduction of the activation energy lead to an increased activity of the innovative catalyst in CO_2 hydrogenation compared to the Graaf catalyst. On the other hand, concerning the reverse Water Gas Shift reaction, the increase of the pre-exponential term and limited decrease of the activation energy seems indicative of an increased production of CO from CO_2 compared to a conventional catalyst.

Table 5: Calibrated pre-exponential term and activation energy of the reaction rate constants of the reactions of CO hydrogenation, RWGS and CO_2 hydrogenation.

Reaction	Parameter	A_{ps}	E_a [kJ kmol^{-1}]
*CO hydrogenation (*Eq. (1)*)*	k_{ps1} [kmol s^{-1}kg^{-1}Pa^{-1}]	0.247	1.133 * 10^5
*RWGS (*Eq. (2)*)*	k_{ps2} [kmol s^{-1}kg^{-1}Pa$^{-0.5}$]	3.054 * 10^6	1.464 * 10^5
*CO_2 hydrogenation (*Eq. (3)*)*	k_{ps3} [kmol s^{-1}kg^{-1}Pa^{-1}]	1.484 * 10^{-3}	8.620 * 10^4

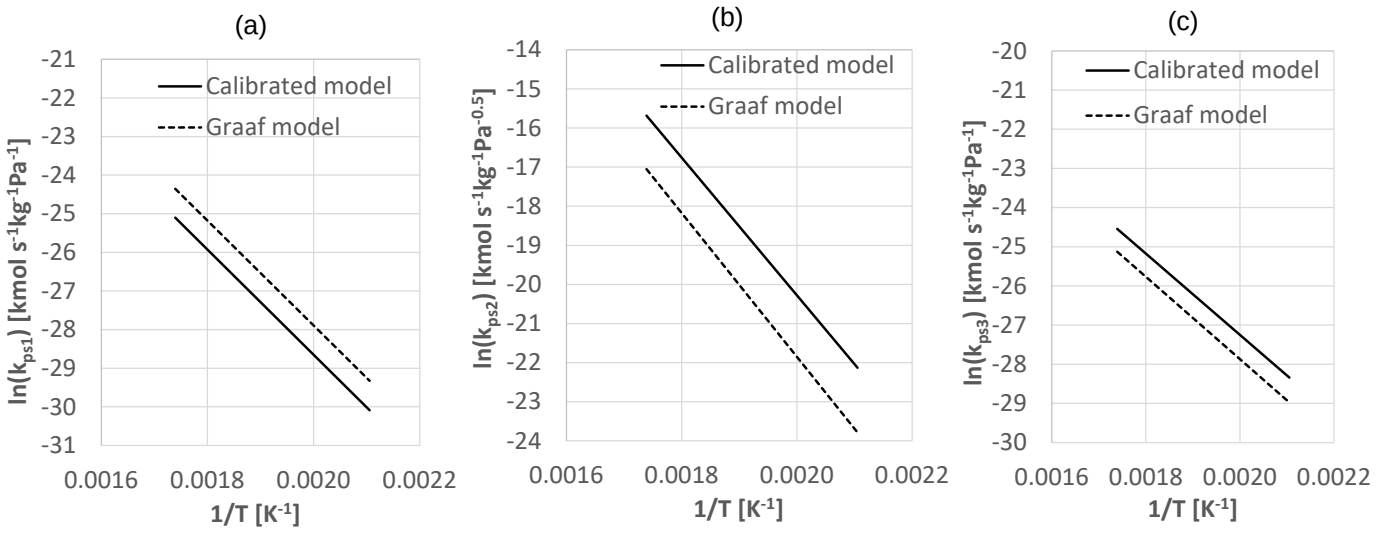

Figure 7: Arrhenius plot of the kinetic constants k_{ps1} (a), k_{ps2} (b) and k_{ps3} (c) for the calibrated model in comparison to those calculated with the Graaf model between 200 °C and 300 °C.

The agreement between experimental results and the calibrated model output can be assessed, also from a graphical point of view, by means of the parity plots reported in *Figure 8*, where the flow rates of CO_2, CO and CH_3OH are compared. The experimental flow rates have been calculated from two measured quantities: the gas-chromatographic composition of each species in the product stream and the gas flow rates

of each component in the inlet stream; the combined uncertainty of the experimental flow rates, evaluated by propagating the uncertainty of each measured quantity, is estimated to be lower or equal to ±2% of the measured value.

The parity plots show that the percentage errors between the simulation and experimental results are less than 10% for all except point #8 (specifically concerning the predicted methanol flow rate, $n_{CH3OH,exp}$ = 3.12 NmL min^{-1}, which is 14% lower than the measured value, $n_{CH3OH,sim}$ = 2.68 NmL min^{-1}) of the fourteen experimental points for all the assessed quantities. As highlighted in *Table 6*, the deviations in terms of molar concentrations between calibrated model predictions and experimental data are limited and ranging between 0 and 0.72 % points; in terms of CO_2 conversion and methanol yields are in the range 0 – 2 % points.

The good agreement between simulations and experimental data reflects the accuracy of the model in the calculation of the mass and energy balances of the synthesis process. Given the reasonable matching between simulations and measured data, the calibrated model represents a valid starting point for future process simulation studies and techno economic analyses of methanol synthesis with the Cu/Zn/Al/Zr catalyst. The model is based on the macro-kinetic approach described by Graaf [45] which, similarly to other well-known models such as Van den Bussche and Froment [52] and Park et al. [49], is widely used for process design and techno-economic assessment purposes (see for instance the study by Kiss et al. [53]). On the other hand, this model is not developed and not suitable for detailed kinetic simulations, where microkinetic models are instead required (see for example the study by Grabow and Mavrikakis [54]).

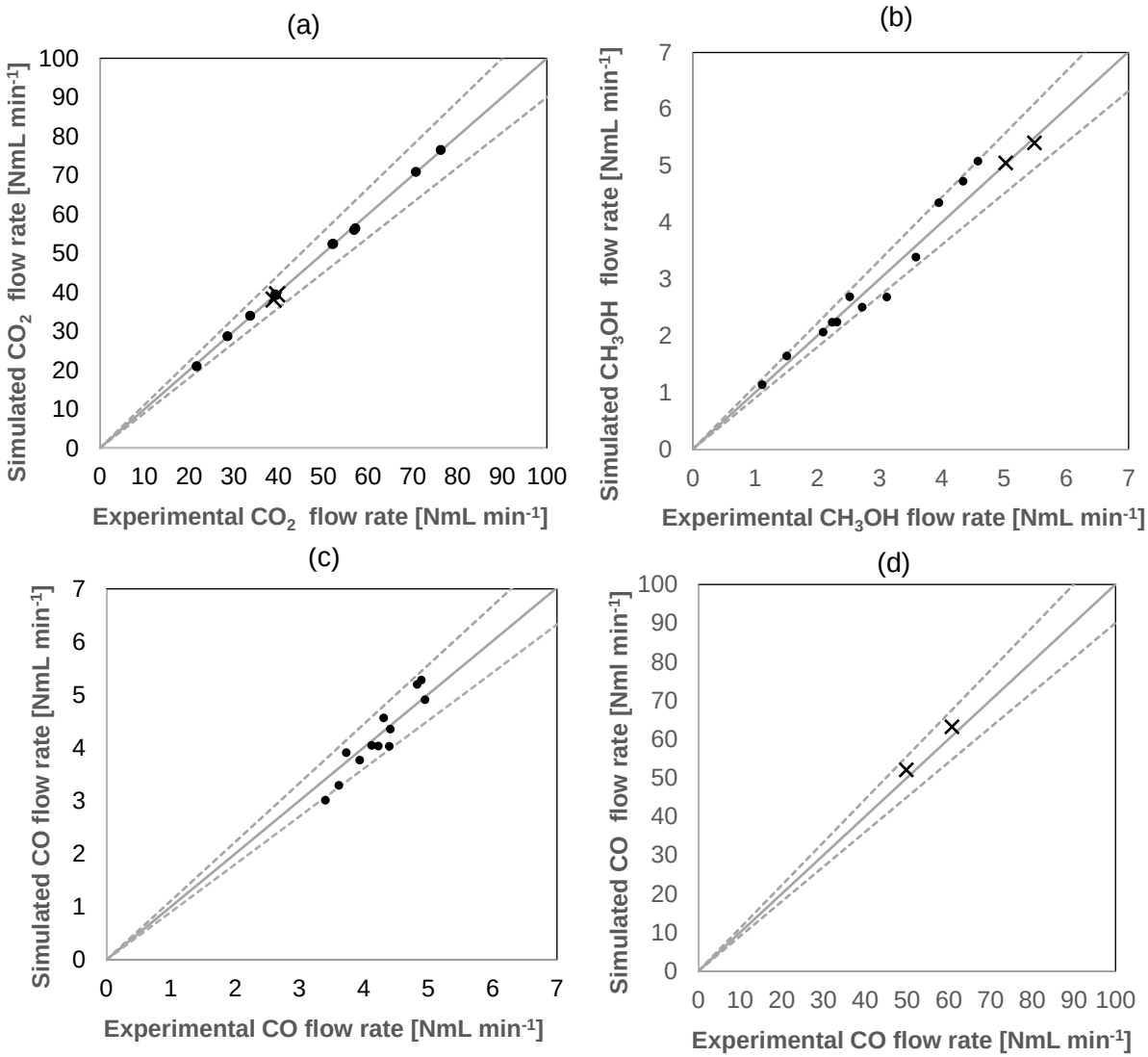

389

390 *Figure 8: Parity plot of simulated vs. experimental flow rates of CO_2 (a), CH_3OH (b) and CO (c-d) for the*

391 *twelve tests of CO_2 hydrogenation (•) and two tests of CO_2/CO hydrogenation (x).*

392

Table 6: Comparison between experimental and simulation results: concentration of CO_2, CO and CH_3OH at reactor outlet, CO_2 conversion (X_{CO2}) and methanol yields (Y_{CH3OH}).

	Experimental results					Calibrated model results				
Test ID#	CO_2 (%mol)	CO (%mol)	CH_3OH (%mol)	X_{CO2} (%)	Y_{CH3OH} (%)	CO_2 (%mol)	CO (%mol)	CH_3OH (%mol)	X_{CO2} (%)	Y_{CH3OH} (%)
1	14.5	1.8	0.77	15.2	4.5	14.6	1.7	0.84	14.7	4.9
2	20.6	1.4	1.04	10.8	4.5	20.6	1.4	0.99	10.5	4.3
3	15.1	1.2	0.67	11.1	3.9	15.1	1.2	0.65	10.7	3.8
4	9.7	1.0	0.32	11.8	2.9	9.8	0.9	0.33	10.9	3.0
5	15.0	1.3	0.65	11.3	3.8	15.2	1.2	0.65	10.7	3.8
6	11.3	1.1	0.61	13.3	4.6	11.4	1.1	0.60	12.9	4.6
7	15.4	0.9	0.55	8.6	3.3	15.5	0.9	0.51	8.2	3.0
8	15.9	0.7	0.48	6.8	2.8	15.9	0.7	0.42	6.6	2.4
9	11.4	1.2	0.73	14.4	5.5	11.4	1.2	0.78	14.6	5.8
10	17.9	1.5	1.36	13.8	6.5	17.8	1.6	1.49	15.0	7.1
11	17.9	1.5	1.44	14.3	6.9	17.7	1.7	1.60	15.6	7.7
12	6.3	1.1	1.16	26.2	13.5	6.2	1.1	1.28	28.2	14.8
13	11.4	14.6	1.47	5.8	5.3	11.2	15.3	1.49	7.7	5.3
14	8.0	12.3	1.11	8.4	5.1	8.1	12.9	1.10	8.9	5.0

5. CONCLUSIONS

In this work, lab-scale tests on an innovative Cu/Zn/Al/Zr catalyst for methanol synthesis are reported, in order to study the catalyst behavior under different operating conditions typical of CO_2 hydrogenation with or without the presence of CO in the feed stream (crucial to simulate the effect of recycle ratio). Fourteen experimental tests covering a wide range of operating conditions relevant to technological application are carried out: temperature always equal to 250 °C, pressure between 3.0 and 7.0 MPa, Gas Hourly Space Velocity in the range 7,000-13,000 h^{-1} and H_2/CO_2 molar ratio between 3 and 6. Experiments, performed in an isothermal fixed-bed reactor with gas chromatographic analysis of the product stream, confirm the improved activity of the catalyst in CO_2 hydrogenation compared to a conventional catalyst, reporting methanol yields between 3 and 13% (the latter corresponding to the case with 7.0 MPa and H_2/CO_2 molar ratio equal to 6).

Moreover, a kinetic model is developed and calibrated on the basis of experimental results. The laboratory reactor is modeled in Aspen Plus as an isothermal pseudo-homogeneous one-dimensional Plug Flow Reactor (PFR) and the reaction rates of the methanol synthesis reactions are described based on a LHHW mechanism as reported in the Graaf's kinetic model. The optimal parameters of the kinetic model are determined with Matlab. The Matlab error minimization routine is coupled with Aspen Plus for the simulation of the reactor

thermo-chemical behavior in order to calculate the mass and energy balance. The calibrated kinetic parameters show an increase of the pre-exponential term and a reduction of the activation energy for the CO_2 hydrogenation reaction compared to the Graaf values, confirming a slightly increased activity of the innovative catalyst in CO_2 hydrogenation. On the other hand, the slight decrease of the activation energy for the reverse Water Gas Shift reaction compared to Graaf catalyst suggests increased selectivity to CO with respect to conventional syngas-to-methanol catalysts.

The calibrated model shows a good agreement between experimental data and simulations, with discrepancies in terms of molar flow rates of CO, CO_2 and CH_3OH lower than 10% of the measured values. Therefore, the identified kinetic parameters represent a valid starting point for future process simulations studies and techno-economic analyses focusing on methanol production from CO_2-rich flows over the novel Cu/Zn/Al/Zr catalyst characterized in this study.

ACKNOWLEDGEMENTS

The Emilia-Romagna Region and the EU are acknowledged for funding the PhD scholarship of Giorgia Lombardelli entitled "*Sviluppo di tecnologie criogeniche per la produzione di biometano liquido a partire da biogas*", Rif. P.A. n° 2018-10680/RER, CUP D36C19000080005 (POR FSE 2014/2020). The Sotacarbo contribution to this work has been funded by *Sardegna Ricerche* within the "Centre of Excellence on Clean Energy" project (CUP: D49J21001310002). The authors are grateful to prof. Elisabetta Rombi (University of Cagliari, Italy) for her valuable contribution on catalysts development and characterization.

Nomenclature

A	A parameter in equilibrium and adsorption equilibrium constants
A_{ps}	Pre-exponential term in rate constants
B	B parameter in equilibrium and adsorption equilibrium constants
E_a	Activation energy [kJ $kmol^{-1}$]
EF	Error function
f_j	Fugacity of component j [Pa]
GHSV	Gas hourly space velocity [h^{-1}]
K_{CO}	Adsorption equilibrium constants of CO [Pa^{-1}]

K_{CO2}	Adsorption equilibrium constants of CO_2 [Pa^{-1}]
$K_{H2O}/K_{H2}^{1/2}$	Adsorption equilibrium constants of H_2O/H_2 [$Pa^{-0.5}$]
K_{p1}	Equilibrium constants of the CO hydrogenation reaction [Pa^{-2}]
K_{p2}	Equilibrium constants of the reverse water-gas shift reaction [-]
K_{p3}	Equilibrium constants of the CO_2 hydrogenation reaction [Pa^{-2}]
k_{ps1}	Rate constant of the CO hydrogenation reaction [kmol $s^{-1}kg^{-1}Pa^{-1}$]
k_{ps2}	Rate constant of the reverse water-gas shift reaction [kmol $s^{-1}kg^{-1}Pa^{-0.5}$]
k_{ps3}	Rate constant of the CO_2 hydrogenation reaction [kmol $s^{-1}kg^{-1}Pa^{-1}$]
$n_{j,exp}$	flow rate of component j at the outlet of the reactor in experiment results [mmol/s]
$n_{j,sim}$	flow rate of component j at the outlet of the reactor in simulation results [mmol/s]
R	Ideal gas constant = 8.314 [J mol^{-1} K^{-1}]
$r_{CH_3OH,CO}$	Rate of reaction of CO hydrogenation [kmol $s^{-1}kg^{-1}$]
$r_{CH_3OH,CO2}$	Rate of reaction of CO_2 hydrogenation [kmol $s^{-1}kg^{-1}$]
r_{H2O}	Rate of reaction of RWGS [kmol $s^{-1}kg^{-1}$]
$x_{j,out}$	Concentration of component j at the outlet of the reactor [-]
$x_{j,in}$	Concentration of component j at the inlet of the reactor [-]
X_{CO2}	CO_2 conversion [%]
Y_{CH3OH}	Methanol yield [%]
$\Delta H^0_{R(298K)}$	Enthalpy of reaction at 298 K and 1 bar (kJ mol^{-1})

REFERENCES

[1] How Methanol is used, (n.d.). https://www.methanex.com/about-methanol/how-methanol-used (accessed June 8, 2022).

[2] J. Nyári, M. Magdeldin, M. Larmi, M. Järvinen, A. Santasalo-Aarnio, Techno-economic barriers of an industrial-scale methanol CCU-plant, J. CO2 Util. 39 (2020). https://doi.org/10.1016/j.jcou.2020.101166.

[3] International Renewable Energy Agency, Methanol Institute, INNOVATION OUTLOOK Renewable Methanol, 2021. https://www.methanol.org/wp-content/uploads/2020/04/IRENA_Innovation_Renewable_Methanol_2021.pdf.

[4] M. Bertau, H. Offermanns, L. Plass, F. Schmidt, H.J. Wernicke, Methanol: The basic chemical and energy feedstock of the future: Asinger's vision today, 2014. https://doi.org/10.1007/978-3-642-39709-7.

[5] M. Bowker, Methanol Synthesis from CO2 Hydrogenation, ChemCatChem. 11 (2019) 4238–4246. https://doi.org/10.1002/cctc.201900401.

[6] J. Zhong, X. Yang, Z. Wu, B. Liang, Y. Huang, T. Zhang, State of the art and perspectives in heterogeneous catalysis of CO2 hydrogenation to methanol, Chem. Soc. Rev. 49 (2020) 1385–1413. https://doi.org/10.1039/c9cs00614a.

[7] M.D. Porosoff, B. Yan, J.G. Chen, Catalytic reduction of CO2 by H2 for synthesis of CO, methanol and hydrocarbons: Challenges and opportunities, Energy Environ. Sci. 9 (2016) 62–73. https://doi.org/10.1039/c5ee02657a.

[8] G.H. Graaf, H. Scholtens, E.J. Stamhuis, A.A.C.M. Beenackers, INTRA-PARTICLE dIFFUSION LIMITATIONS IN LOW-PRESSURE METHANOL SYNTHESIS, Chem. Eng. Sci. 45 (1990) 773–783.

[9] S. Dehghanpoor, M.H. Sedaghat, A. Bakhtyari, M.A. Makarem, M.R. Rahimpour, A Feasibility Study of the Conversion of Petrochemical Off-Gas Streams to Methanol Over CuO/ZnO/Al2O3 Catalyst, Top. Catal. (2022). https://doi.org/10.1007/s11244-022-01570-0.

[10] S.A. Ning Asih, A. Syauqi, W.W. Purwanto, Techno-enviro-economic analysis of integrated direct chemical looping coal-based power generation and methanol synthesis using renewable hydrogen, J. CO2 Util. 54 (2021) 101768. https://doi.org/10.1016/j.jcou.2021.101768.

[11] M.M. Zain, A.R. Mohamed, An overview on conversion technologies to produce value added products from CH4 and CO2 as major biogas constituents, Renew. Sustain. Energy Rev. 98 (2018) 56–63. https://doi.org/10.1016/j.rser.2018.09.003.

[12] C. Hank, S. Gelpke, A. Schnabl, R.J. White, J. Full, N. Wiebe, T. Smolinka, A. Schaadt, H.M. Henning, C. Hebling, Economics & carbon dioxide avoidance cost of methanol production based on renewable hydrogen and recycled carbon dioxide-power-to-methanol, Sustain. Energy Fuels. 2 (2018) 1244–1261. https://doi.org/10.1039/c8se00032h.

[13] M. Rivarolo, D. Bellotti, L. Magistri, A.F. Massardo, Feasibility study of methanol production from different renewable sources and thermo-economic analysis, Int. J. Hydrogen Energy. 41 (2016) 2105–2116. https://doi.org/10.1016/j.ijhydene.2015.12.128.

[14] A.D.N. Kamkeng, M. Wang, J. Hu, W. Du, F. Qian, Transformation technologies for CO2 utilisation: Current status, challenges and future prospects, Chem. Eng. J. 409 (2021) 128138. https://doi.org/10.1016/j.cej.2020.128138.

[15] Global CO2 Initiative, CO2 Sciences Inc., Global Roadmap for Implementing CO2 Utilization, Report. (2016) 20534. https://assets.ctfassets.net/xg0gv1arhdr3/27vQZEvrxaQiQEAsGyoSQu/44ee0b72ceb9231ec53ed180cb759614/CO2U_ICEF_Roadmap_FINAL_2016_12_07.pdf.

[16] G. Harp, K.C. Tran, C. Bergins, T. Buddenberg, I. Drach, O. Sigurbjornsson, C. Bergins, M. Hitachi, P. Systems, E. Gmbh, Application of Power to Methanol Technology to Integrated Steelworks for Profitability , Conversion Efficiency , and CO 2 Reduction . Contact : The Power to Methanol (PtMeOH) Concept CRI ' s Production of Methanol, METEC 2nd ESTAD, Düsseldorf, Ger. (2016) 15–19.

[17] D.S. Marlin, E. Sarron, Ó. Sigurbjörnsson, Process Advantages of Direct CO2 to Methanol Synthesis, Front. Chem. 6 (2018) 1–8. https://doi.org/10.3389/fchem.2018.00446.

[18] V. Dieterich, A. Buttler, A. Hanel, H. Spliethoff, S. Fendt, Power-to-liquid via synthesis of methanol, DME or Fischer–Tropsch-fuels: a review, Energy Environ. Sci. 13 (2020) 3207–3252. https://doi.org/10.1039/d0ee01187h.

[19] F. Nestler, A.R. Schütze, M. Ouda, M.J. Hadrich, A. Schaadt, S. Bajohr, T. Kolb, Kinetic modelling of

methanol synthesis over commercial catalysts: A critical assessment, Chem. Eng. J. 394 (2020). https://doi.org/10.1016/j.cej.2020.124881.

[20] B. Liang, J. Ma, X. Su, C. Yang, H. Duan, H. Zhou, S. Deng, L. Li, Y. Huang, Investigation on Deactivation of Cu/ZnO/Al2O3 Catalyst for CO2 Hydrogenation to Methanol, Ind. Eng. Chem. Res. 58 (2019) 9030–9037. https://doi.org/10.1021/acs.iecr.9b01546.

[21] J. Wang, G. Li, Z. Li, C. Tang, Z. Feng, H. An, H. Liu, T. Liu, C. Li, A highly selective and stable ZnO-ZrO2 solid solution catalyst for CO2 hydrogenation to methanol, Sci. Adv. 3 (2017) 1–11. https://doi.org/10.1126/sciadv.1701290.

[22] E.C. Ra, K.Y. Kim, E.H. Kim, H. Lee, K. An, J.S. Lee, Recycling Carbon Dioxide through Catalytic Hydrogenation: Recent Key Developments and Perspectives, ACS Catal. 10 (2020) 11318–11345. https://doi.org/10.1021/acscatal.0c02930.

[23] S.G. Jadhav, P.D. Vaidya, B.M. Bhanage, J.B. Joshi, Catalytic carbon dioxide hydrogenation to methanol: A review of recent studies, Chem. Eng. Res. Des. 92 (2014) 2557–2567. https://doi.org/10.1016/j.cherd.2014.03.005.

[24] M.M.J. Li, S.C.E. Tsang, Bimetallic catalysts for green methanol production via CO2 and renewable hydrogen: A mini-review and prospects, Catal. Sci. Technol. 8 (2018) 3450–3464. https://doi.org/10.1039/c8cy00304a.

[25] A. Alavarez, A. Bansode, A. Urakawa, A. V Bavykina, T.A. Wezendonk, M. Makkee, J. Gascon, F. Kapteijn, Challenges in the Greener Production of Formates / Formic Acid , Methanol , and DME by Heterogeneously Catalyzed CO2 Hydrogenation Processes, (2017). https://doi.org/10.1021/acs.chemrev.6b00816.

[26] C. Yang, Z. Ma, N. Zhao, W. Wei, T. Hu, Y. Sun, Methanol synthesis from CO2-rich syngas over a ZrO2 doped CuZnO catalyst, Catal. Today. 115 (2006) 222–227. https://doi.org/10.1016/j.cattod.2006.02.077.

[27] S. Xiao, Y. Zhang, P. Gao, L. Zhong, X. Li, Z. Zhang, H. Wang, W. Wei, Y. Sun, Highly efficient Cu-based catalysts via hydrotalcite-like precursors for CO2 hydrogenation to methanol, Catal. Today. 281 (2017) 327–336. https://doi.org/10.1016/j.cattod.2016.02.004.

[28] C. Paris, A. Karelovic, R. Manrique, S. Le Bras, F. Devred, V. Vykoukal, A. Styskalik, P. Eloy, D.P. Debecker, CO2 Hydrogenation to Methanol with Ga- and Zn-Doped Mesoporous Cu/SiO2 Catalysts Prepared by the Aerosol-Assisted Sol-Gel Process**, ChemSusChem. 13 (2020) 6409–6417. https://doi.org/10.1002/cssc.202001951.

[29] M.M.J. Li, C. Chen, T. Ayvall, H. Suo, J. Zheng, I.F. Teixeira, L. Ye, H. Zou, D. O'Hare, S.C.E. Tsang, CO2 Hydrogenation to Methanol over Catalysts Derived from Single Cationic Layer CuZnGa LDH Precursors, ACS Catal. 8 (2018) 4390–4401. https://doi.org/10.1021/acscatal.8b00474.

[30] C. Li, X. Yuan, K. Fujimoto, Development of highly stable catalyst for methanol synthesis from carbon dioxide, Appl. Catal. A Gen. 469 (2014) 306–311. https://doi.org/10.1016/j.apcata.2013.10.010.

[31] S. Ghosh, J. Sebastian, L. Olsson, D. Creaser, Experimental and kinetic modeling studies of methanol synthesis from CO2 hydrogenation using In2O3 catalyst, Chem. Eng. J. 416 (2021) 129120. https://doi.org/10.1016/j.cej.2021.129120.

[32] P. Gao, L. Zhong, L. Zhang, H. Wang, N. Zhao, W. Wei, Y. Sun, Yttrium oxide modified Cu/ZnO/Al2O3 catalysts via hydrotalcite-like precursors for CO2 hydrogenation to methanol, Catal. Sci. Technol. 5 (2015) 4365–4377. https://doi.org/10.1039/c5cy00372e.

[33] W. Cai, P.R. De La Piscina, J. Toyir, N. Homs, CO<inf>2</inf> hydrogenation to methanol over CuZnGa catalysts prepared using microwave-assisted methods, Catal. Today. 242 (2015) 193–199.

https://doi.org/10.1016/j.cattod.2014.06.012.

[34] H. Bahruji, M. Bowker, W. Jones, J. Hayward, J. Ruiz Esquius, D.J. Morgan, G.J. Hutchings, PdZn catalysts for CO2 hydrogenation to methanol using chemical vapour impregnation (CVI), Faraday Discuss. 197 (2017) 309–324. https://doi.org/10.1039/c6fd00189k.

[35] X. AN, Y. ZUO, Q. ZHANG, J. WANG, Methanol Synthesis from CO2 Hydrogenation with a Cu/Zn/Al/Zr Fibrous Catalyst, Chinese J. Chem. Eng. 17 (2009) 88–94. https://doi.org/10.1016/S1004-9541(09)60038-0.

[36] F.C.F. Marcos, F.M. Cavalcanti, D.D. Petrolini, L. Lin, L.E. Betancourt, S.D. Senanayake, J.A. Rodriguez, J.M. Assaf, R. Giudici, E.M. Assaf, Effect of operating parameters on H2/CO2 conversion to methanol over Cu-Zn oxide supported on ZrO2 polymorph catalysts: Characterization and kinetics, Chem. Eng. J. 427 (2022). https://doi.org/10.1016/j.cej.2021.130947.

[37] X.M. Liu, G.Q. Lu, Z.F. Yan, J. Beltramini, Recent Advances in Catalysts for Methanol Synthesis via Hydrogenation of CO and CO2, Ind. Eng. Chem. Res. 42 (2003) 6518–6530. https://doi.org/10.1021/ie020979s.

[38] H.W. Lim, M.J. Park, S.H. Kang, H.J. Chae, J.W. Bae, K.W. Jun, Modeling of the kinetics for methanol synthesis using Cu/ZnO/Al 2O3/ZrO2 catalyst: Influence of carbon dioxide during hydrogenation, Ind. Eng. Chem. Res. 48 (2009) 10448–10455. https://doi.org/10.1021/ie901081f.

[39] M. Mureddu, S. Lai, L. Atzori, E. Rombi, F. Ferrara, A. Pettinau, M.G. Cutrufello, Ex-ldh-based catalysts for co2 conversion to methanol and dimethyl ether, Catalysts. 11 (2021). https://doi.org/10.3390/catal11050615.

[40] J.F. Portha, K. Parkhomenko, K. Kobl, A.C. Roger, S. Arab, J.M. Commenge, L. Falk, Kinetics of Methanol Synthesis from Carbon Dioxide Hydrogenation over Copper-Zinc Oxide Catalysts, Ind. Eng. Chem. Res. 56 (2017) 13133–13145. https://doi.org/10.1021/acs.iecr.7b01323.

[41] P. Gao, R. Xie, H. Wang, L. Zhong, L. Xia, Z. Zhang, W. Wei, Y. Sun, Cu / Zn / Al / Zr catalysts via phase-pure hydrotalcite-like compounds for methanol synthesis from carbon dioxide, 11 (2015) 41–48.

[42] M. Mureddu, F. Ferrara, A. Pettinau, Highly efficient CuO/ZnO/ZrO2@SBA-15 nanocatalysts for methanol synthesis from the catalytic hydrogenation of CO2, Appl. Catal. B Environ. 258 (2019). https://doi.org/10.1016/j.apcatb.2019.117941.

[43] K. Atsonios, K.D. Panopoulos, E. Kakaras, Investigation of technical and economic aspects for methanol production through CO2 hydrogenation, Int. J. Hydrogen Energy. 41 (2016) 2202–2214. https://doi.org/10.1016/j.ijhydene.2015.12.074.

[44] P. Battaglia, G. Buffo, D. Ferrero, M. Santarelli, A. Lanzini, Methanol synthesis through CO2capture and hydrogenation: Thermal integration, energy performance and techno-economic assessment, J. CO2 Util. 44 (2021). https://doi.org/10.1016/j.jcou.2020.101407.

[45] G.H. Graaf, E.J. Stamhuis, A.A.C.M. Beenackers, KINETICS OF LOW-PRESSURE METHANOL SYNTHESIS, Chem. Eng. Sci. 43 (1988) 3185–3195.

[46] D. Izbassarov, J. Nyári, B. Tekgül, E. Laurila, T. Kallio, A. Santasalo-Aarnio, O. Kaario, V. Vuorinen, A numerical performance study of a fixed-bed reactor for methanol synthesis by CO2 hydrogenation, Int. J. Hydrogen Energy. 46 (2021) 15635–15648. https://doi.org/10.1016/j.ijhydene.2021.02.031.

[47] Y. Slotboom, M.J. Bos, J. Pieper, V. Vrieswijk, B. Likozar, S.R.A. Kersten, D.W.F. Brilman, Critical assessment of steady-state kinetic models for the synthesis of methanol over an industrial Cu/ZnO/Al2O3 catalyst, Chem. Eng. J. 389 (2020). https://doi.org/10.1016/j.cej.2020.124181.

[48] G.H. Graaf, P.J.J.M. Sijtsema, E.J. Stamhuis, G.E.H. Joosten, Chemical equilibria in methanol synthesis, Chem. Eng. Sci. 41 (1986) 2883–2890. https://doi.org/10.1016/0009-2509(86)80019-7.

[49] N. Park, M.J. Park, Y.J. Lee, K.S. Ha, K.W. Jun, Kinetic modeling of methanol synthesis over commercial catalysts based on three-site adsorption, Fuel Process. Technol. 125 (2014) 139–147. https://doi.org/10.1016/j.fuproc.2014.03.041.

[50] Z. Liang, P. Gao, Z. Tang, M. Lv, Y. Sun, Three dimensional porous Cu-Zn/Al foam monolithic catalyst for CO2 hydrogenation to methanol in microreactor, J. CO2 Util. 21 (2017) 191–199. https://doi.org/10.1016/j.jcou.2017.05.023.

[51] C. Cara, F. Secci, S. Lai, V. Mameli, K. Skrodczky, P.A. Russo, F. Ferrara, E. Rombi, N. Pinna, M. Mureddu, C. Cannas, On the design of mesostructured acidic catalysts for the one-pot dimethyl ether production from CO2, J. CO2 Util. 62 (2022) 102066. https://doi.org/10.1016/j.jcou.2022.102066.

[52] K.M. Vanden Bussche, G.F. Froment, A steady-state kinetic model for methanol synthesis and the water gas shift reaction on a commercial Cu/ZnO/Al2O3 catalyst, J. Catal. 161 (1996) 1–10.

[53] A.A. Kiss, J.J. Pragt, H.J. Vos, G. Bargeman, M.T. de Groot, Novel efficient process for methanol synthesis by CO2 hydrogenation, Chem. Eng. J. 284 (2016) 260–269. https://doi.org/10.1016/j.cej.2015.08.101.

[54] L.C. Grabow, M. Mavrikakis, Mechanism of methanol synthesis on cu through CO2 and CO hydrogenation, ACS Catal. 1 (2011) 365–384. https://doi.org/10.1021/cs200055d.